

Super-resolution of hyperspectral images using local spectral unmixing

Giorgio Antonino Licciardi, Miguel Angel Veganzones, Miguel Simoes, José M. Bioucas-Dias, Jocelyn Chanussot

▶ **To cite this version:**

Giorgio Antonino Licciardi, Miguel Angel Veganzones, Miguel Simoes, José M. Bioucas-Dias, Jocelyn Chanussot. Super-resolution of hyperspectral images using local spectral unmixing. WHISPERS 2014 - 6th Workshop on Hyperspectral Image and Signal Processing: Evolution in Remote Sensing, Jun 2014, Lausanne, Switzerland. pp.n/c. hal-01010428

HAL Id: hal-01010428
https://hal.science/hal-01010428

Submitted on 19 Jun 2014

HAL is a multi-disciplinary open access archive for the deposit and dissemination of scientific research documents, whether they are published or not. The documents may come from teaching and research institutions in France or abroad, or from public or private research centers.

L'archive ouverte pluridisciplinaire **HAL**, est destinée au dépôt et à la diffusion de documents scientifiques de niveau recherche, publiés ou non, émanant des établissements d'enseignement et de recherche français ou étrangers, des laboratoires publics ou privés.

SUPER-RESOLUTION OF HYPERSPECTRAL IMAGES USING LOCAL SPECTRAL UNMIXING

G. Licciardi[1], M.A. Veganzones[1], M. Simões[1,2], J. Bioucas[2], J. Chanussot[1,3].

1 GIPSA-lab, Grenoble-INP, Saint Martin d'Hères, France
2 Instituto de Telecomunicações, Instituto Superior Técnico, Lisbon, Portugal
3 Faculty of Electrical and Computer Engineering, University of Iceland, Reykjavik, Iceland

ABSTRACT

For many remote sensing applications it is preferable to have images with both high spectral and spatial resolutions. On this regards, hyperspectral and multispectral images have complementary characteristics in terms of spectral and spatial resolutions. In this paper we propose an approach for the fusion of low spatial resolution hyperspectral images with high spatial resolution multispectral images in order to obtain super-resolution (spatial and spectral) hyperspectral images. The proposed approach is based on the assumption that, since both hyperspectral and multispectral images acquired on the same scene, the corresponding endmembers should be the same. On a first step the hyperspectral image is spectrally down-sampled in order to match the multispectral one. Then an endmember extraction algorithm is performed on the down-sampled hyperspectral image and the successive abundance estimation is performed on the multispectral one. Finally, the extracted endmembers are up-sampled back to the original hyperspectral space and then used to reconstruct the super-resolution hyperspectral image according to the abundances obtained from the multispectral image.

Index Terms— hyperspectral imaging, super-resolution, spectral unmixing.

1. INTRODUCTION

Many efforts have been spent in the last decades to improve the spectral and spatial resolutions of remote sensing sensors. However, there are design constraints that result in an inverse relation between spatial and spectral resolution. Moreover, the system trade-off related to data volume and signal-to-noise ratio (SNR) limitations prevent to achieve both of them simultaneously. Many practical applications require images having both high spectral and spatial resolution. Thus, there is a need for techniques that fuse high spectral resolution images, such as hyperspectral images (HS), with high spatial images such as multispectral images (MS) or panchromatic images (PAN), in order to obtain high spectral and spatial (super-resolution) images. In the literature there exist many applications combining hyperspectral and panchromatic images [1]. These techniques, that goes under the name of pan-sharpening, are considered adequate when applied to multispectral and PAN images, but have many drawbacks when the low-resolution image is a hyperspectral image [2]. Recently, some techniques dedicated to the fusion of hyperspectral images and multispectral ones have been proposed [3][4][5]. In general, the approach is to associate the fusion problem with linear spectral unmixing, which assumes that the underlying data can be described by a mixture of a relatively small number of pure spectral signatures, corresponding to the materials present in the scene. Since both hyperspectral and multispectral images capture the same scene, the endmembers should be the same. Therefore, the spectral information extracted from one of the images should also be able to explain the other one. Due to the high spectral resolution of a hyperspectral image, the endmembers can be extracted from this data, and then used to reconstruct the multispectral image. Since the multispectral image have high spatial resolution, the final reconstructed image will be at super-resolution. In [4] the same approach has been followed with the only difference that the mixing matrix is replaced by a dictionary learnt using a non-negative matrix factorization with sparsity regularization on the code. In [5], the hyperspectral data is unmixed via the K-SVD algorithm, and the multispectral data is reconstructed using orthogonal matching pursuit to induce sparsity. In [6] alternately unmixes both sources of data to find the signatures and the abundances of the endmembers, while in [3] two dictionaries were learned from the two different data, and then used a dictionary-pair learning method to establish the correspondence between them.

However, the effectiveness of these approaches strongly depends on how the dictionaries can be obtained. In this paper we propose an approach where the endmembers are extracted directly from the spectrally down-sampled hyperspectral image. The derived endmembers are used as input to an unmixing algorithm applied to the multispectral image. The obtained abundances are then used to reconstruct the super-resolution hyperspectral image. This approach permits to reduce the spectral distortion of the enhanced image. The re-

mainder of the paper is organized as follows: in Sec. 2 the proposed super-resolution methodology is introduced and in Sec. 4 experimental results are presented. Finally in Sec. 5 conclusion remarks are provided.

2. HYPERSPECTRAL SUPER RESOLUTION

In order to better understand the proposed approach,we define $X \in \mathbb{R}^{m \times n}$ as the super-resolution hyperspectral image having m spectral bands and n pixels. In this way it is possible to define the hyperspectral image Y_h as the spatial degradation of X:

$$Y_h = XBM + N_h \tag{1}$$

where B is a matrix modeling band independent sensor blur, M is a masking matrix accounting for spatial downsampling and N_h is an additive perturbation. In a similar way the multispectral image Y_m can be defined as the spectral degradation of$X$:

$$Y_m = RX + N_m \tag{2}$$

where the matrix R models the spectral responses of the multispectral sensor, and N_m is an additive perturbation. If it is possible to learn a dictionary D from the hyperspectral image Y_h, then each pixel x_i (for $i = 1, ...n$) of X can be represented as a linear combination of the elements of D:

$$X = DA \tag{3}$$

where $A = [\alpha_1, ..., \alpha_n]$ is defined as the code of the dictionary. Substituting Eq. (3) in Eq. (2), we obtain:

$$Y_m = RDA + N_m \tag{4}$$

If equation (4) can be solved with respect to A, then we may plug its solution into (3) and thereby obtain an estimate of X.

As it can be noted, the quality of the super-resolution image can be strongly influenced by the dictionary. In particular, the elements of the dictionary D should be consistent with the multispectral image Y_m. This means that, since the elements of D are derived from Y_h, to match the spectral resolution of Y_m they should be spectrally downsampled. It is then easy to understand that the spectral downsampling of the dictionary is a critical point in terms of quality of the super-resolution image. From a practical point of view, the elements of the dictionary D correspond to the endmembers extracted from the spectrally downsampled hyperspectral image. However, a not perfect model of the spectral responses of the sensors may lead to endmembers that could not match the endmembers extracted from the multispectral image. Thus, is desirable to have endmembers can be extracted directly from Y_h in order to reduce the spectral distortion of the super resolution image.

Another critical point is related to the fact that the product RD may lead to an undetermined system of equations. This because the number of elements of the dictionary D may be higher than the number of spectral bands of Y_m. However, the images are locally low rank, meaning that in a small spatial area the subspace dimensionality is low enough to be represented by a number of elements of D lower than the number of bands of Y_m.

To overcome these problems, in this paper we propose propose a local approach where the images are partitioned into patches. Then the endmembers are extracted independently from each patch. The abundance estimation is then performed on Y_m using the elements of the local dictionary obtained for each patch. In particular, given a set of patches $P_j, j = 1; ...; P$; for each P_j , we identify a mixing matrix D_j by means of the NFINDR algorithm in order to extract a set of endmembers from each patch [7]. Once determined the local dictionary D_j, the code A is estimated by solving the following constrained least squares (CLS) problems:

$$min_{A_j > 0} \|Y_{m,j} - RD_jA_j\|_F^2 \tag{5}$$

where A_j and $Y_{m,j}$ represent the columns of A and Y_m, respectively, with indices corresponding to the pixels X_j in P_j, while $\|\cdot\|_F$ denotes the Frobenius norm. In order to solve (5), we use the SUnSAL algorithm [8] to effectively solve a large number of constrained least squares problems sharing the same matrix system. Once the abundances have been found, the super-resolution hyperspectral image can be retrieved by substituting the hyperspectral endmembers corresponding to the local endmembers found in each patch.

3. EXPERIMENTAL RESULTS

In this section, the proposed method has been applied to two real datasets. The super-resolution images obtained in both experiments will be quantitatively evaluated by means of Relative Dimensional Global Error (ERGAS) and Spectral Angle Mapper (SAM) quality indexes. ERGAS and SAM will both produce positive values with an ideal value of 0. However, values that are around 3 are referred to a good image enhancement. SAM is a useful measure of the spectral quality introduced by the fusion process, while ERGAS measure both spectral and spatial quality. A qualitative analysis, through visual inspection, will also be discussed.

3.1. Hyperion-ALI

On a first experiment the super-resolution image has been obtained by fusing Hyperion and ALI images, both carried by the EO-1 satellite and acquired simultaneously over the city of Paris. Hyperion is a grating imaging spectrometer providing 242 hyperspectral bands (from 0.4 to 2.5 μm) with a 30

meter spatial resolution. The ALI instrument provides 9 spectral bands (from 0.43 to 2.35 μm) with 30-meter resolution. Since the two sensors are carried by the same satellite, and the images are acquired simultaneously, then the super-resolution image will not be affected by differences in terms of angle of view, atmospherical path, illumination as well as misregistration. Moreover, in order to evaluate the method following the "Wald" protocol [9], the Hyperion image has been degraded to a lower resolution, so that the resultant super-resolution image is at the same resolution as the starting reference and hence statistical analysis can be made between the reference and the super-resolution images.

Given the Hyperion image, we simulate a low-spatial resolution hyperspectral image Y_h, by applying a Gaussian blurring (B) and downsampling the blurred image by a factor of four (M). A spectrally downsampled image Y_{hd} is obtained applying the spectral responses models R to Y_h in order to match the spectral resolution of the ALI image Y_m. A sliding window of a fixed size is then defined so that the pixels lying inside the window form a patch. In order to assess the proposed method, different window sizes have been evaluated. Then, for each patch we extracted a set of 10 local endmembers from the spectrally downsampled image Y_{hd} through the use of NFINDR algorithm. The abundances are then estimated by solving Eq. (5). Finally, the fractional abundances are linearly combined with the corresponding endmember of Y_h and the super-resolution pixels are obtained for each patch. For sake of comparisons, the performances of the proposed local method have been compared with those obtained with the same approach but applied globally. Quantitative results are reported in table 1 in terms of SAM and ERGAS measures as the size of the patches changes. As expected, the quality of the super resolution image increases as the size of the patch decreases. However, on a qualitative analysis of the images in Fig. 1, it can be also noted that the image obtained with a 10x10 patch size seems to be the most affine with the reference image.

3.2. Hyperion-ASTER

On a second experiment data fusion was applied to Hyperion and ASTER images taken over San Francisco on 31 July, 2002. ASTER sensor provides images in 14 spectral bands (from 0.52 to 11.65 μm) with spatial resolutions between 15 to 90 meters. However, due to the differences in spectral coverages, only the first three bands of ASTER (0.52 to 0.860 μm), with 15 m ground sampling distance, were used for the fusion. Moreover, we used a Hyperion/VNIR dataset having30 m ground sampling distance and 50 bands (0.43 to 0.92 μm). Since the two images are already at different spatial resolution, a further reduction of the Hyperion image to a lower resolution will lead to no significant information left. For this reason we preferred to not perform any downsampling of the hyperspectral image in order to avoid further distortions.

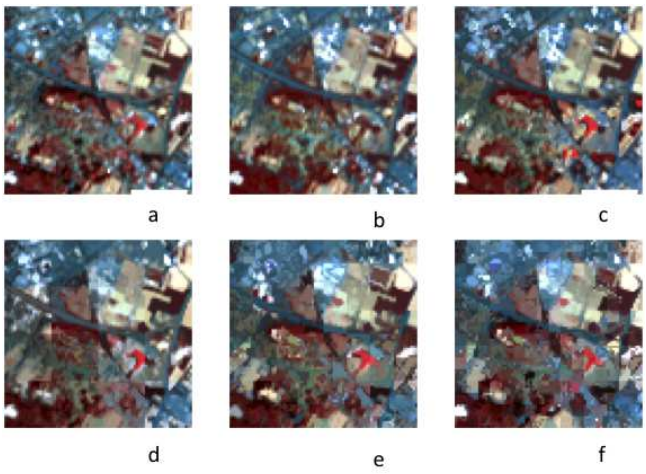


Fig. 1. *Hyperion-ALI dataset: False-color images of the original hyperspectral image (a), and the super-resolution images obtained with the proposed approach on the whole image (b) and with a patch size of 40x40 (c), 20x20 (d), 10x10 (e) and 5x5 (f), respectively.*

Similarly to the previous experiment, the proposed super-resolution method is applied both locally and globally. However, in this case, since the number of bands of the multispectral image is limited to three, we set the number of endmembers to be extracted from the spectrally downsampled image Y_{hd} to 4. From a quantitative point of view, analyzing the values in table 1, it is possible to affirm that he quality of the super resolution image increases as the size of the patch decreases. A further analysis has also been conducted on two different test areas characterized by different spectral features. In particular, the test area 1 is characterized by few spectral endmembers, while test area 2 presents several spectrally different elements. Analyzing the quality indexes in table 1, it can be noted that the best results are obtained on test area 1. This is also evident by analyzing the images in Fig. 1, where the super resolution image relative to the test area 2 is spectrally consistent with the original one but on the other hand, is not as sharp as expected. This problem may be explained by analyzing the spectral separability of the pixels within each patch. In particular, if a patch presents homogeneous pixels, the extracted endmembers may be very similar, and the resulting super-resolution pixels will have very similar values.

	Global	40x40	20x20	10x10	5x5
ERGAS	3.3276	4.4785	4.3290	3.1335	1.1895
SAM	3.4763	2.8132	2.6104	2.4523	2.1392

Table 1. Hyperion-ALI dataset: ERGAS and SAM quality indexes for the super-resolution images obtained using the global and local version of the proposed approach as the size of the patches change.

4. CONCLUSIONS

In this paper we have presented an approach for the super-resolution of hyperspectral images by fusing them with multispectral images. Since both hyperspectral and multispectral images capture the same scene, they should also be able to detect the same endmembers with different spectral resolutions. Based on this assumption, spectrally downsample hyperspectral endmembers should then correspond to the multispectral endmembers. In this work NFINDR was used to extract a set of endmembers from the Spectrally downsample hyperspectral image while the abundance are obtained by solving a constrained least squares problem applied to the multispectral image. In order to improve the quality of super-resolution images and also to avoid that the number of endmembers may be higher than the number of spectral bands , we proposed a local approach, where the images are partitioned into patches and the method is applied independently on each patch. Experiments on two real datasets demonstrate the effectiveness of the proposed approach to produce super resolution hyperspectral images with low spectral distortion and spatially consistent.

	Global	50x50	25x25	10x10	5x5
Complete image					
ERGAS	8.1943	7.0391	5.3764	3.5339	2.4634
SAM	9.4422	8.3400	6.1084	3.5651	2.2675
Test area 1					
ERGAS	8.1943	4.9006	3.5222	6.8840	1.8681
SAM	8.6509	5.1341	3.2178	2.3629	1.5009
Test area 2					
ERGAS	11.8908	11.0363	9.8373	3.5339	4.8053
SAM	10.7797	10.1970	8.7004	5.0406	2.9463

Table 2. Hyperion-ASTER dataset: ERGAS and SAM quality indexes for the super-resolution images obtained using the global and local version of the proposed approach as the size of the patches change.

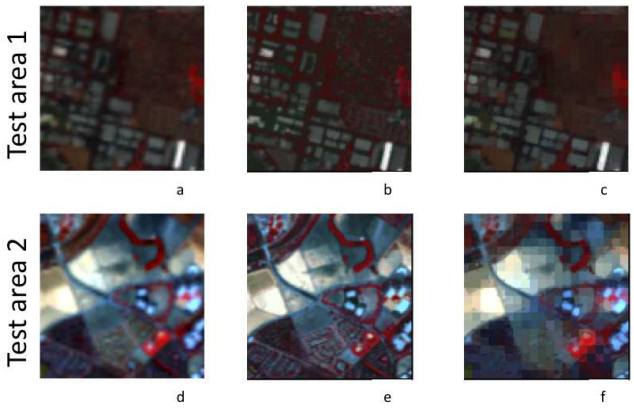


Fig. 2. *Hyperion-ASTER dataset: False-color images obtained using the original hyperspectral image (a, d), and the super resolution image obtained with the proposed method on the whole test areas (b, e), and using a 5x5 patch size (c, f), respectively, for the test area 1 and 2.*

5. REFERENCES

[1] L. Alparone, L. Wald, J. Chanussot, C. Thomas, P. Gamba, and L. M. Bruce, "Comparison of pansharpening algorithms: Outcome of the 2006 grs-s data fusion contest," *IEEE Trans. Geosci. Remote Sens.*, vol. 45, pp. 3012–3021, 2007.

[2] G. Licciardi, M. M. Khan, J. Chanussot, A. Montanvert, L. Condat, and C. Jutten, "Fusion of hyperspectral and panchromatic images using multiresolution analysis and nonlinear pca band reduction," *EURASIP Journal on Advances in Signal Processing*, vol. 4885, no. 8, pp. 347–358, 2012.

[3] H. Song, B. Huang, K. Zhang, and H. Zhang, "Spatio-spectral fusion of satellite images based on dictionary-pair learning," *Information Fusion*, vol. 18, pp. 148–160, 2014.

[4] S. Charles, B. A. Olshausen, and C. J. Rozell, "Learning sparse codes for hyperspectral imagery," *IEEE Journal of Selected Topics in Signal Processing*, vol. 5, pp. 963–978, 2011.

[5] B. Huang, H. Song, H. Cui, J. Peng, and Z. Xu, "Spatial and spectral image fusion using sparse matrix factorization," *IEEE Trans. Geosci. Remote Sens.*, vol. 52, pp. 1693–1704, 2014.

[6] N. Yokoya, T. Yairi, and A. Iwasaki, "Coupled nonnegative matrix factorization unmixing for hyperspectral and multispectral data fusion," *IEEE Trans. Geosci. Remote Sens.*, vol. 50, pp. 528–537, 2012.

[7] Winter M. E., "N-findr: an algorithm for fast autonomous spectral end-member determination in hyperspectral data," *Proc. SPIE*, vol. 3753, pp. 266–275, 1999.

[8] J. M. Bioucas-Dias and M. A. Figueiredo, "Alternating direction algorithms for constrained sparse regression: Application to hyperspectral unmixing," *IEEE 2nd WHISPERS Workshop*, pp. 1–4, 2010.

[9] L. Wald, "Data fusion. definitions and architectures - fusion of images of different spatial resolutions," *Presses de l'Ecole, Ecole des Mines de Paris, Paris, France*, 2002.